ISSN 1674-1056
http://cpb.iphy.ac.cn
http://iopscience.iop.org/cpb
中国物理 B
Chinese Physics
中国物理
Chinese Physics B

Characterization of inner layer thickness change of a composite circular tube using nonlinear circumferential guided wave: A feasibility study

Ming-Liang Li(李明亮), Guang-Jian Gao(高广健), and Ming-Xi Deng(邓明晰)
Citation: Chin. Phys. B, 2021, 30 (**8**): 084301. DOI: 10.1088/1674-1056/abe234
Journal homepage: http://cpb.iphy.ac.cn; http://iopscience.iop.org/cpb

What follows is a list of articles you may be interested in

An ultrasonic multi-wave focusing and imaging method for linear phased arrays

Yu-Xiang Dai(戴宇翔), Shou-Guo Yan(阎守国), and Bi-Xing Zhang(张碧星)
Chin. Phys. B, 2021, 30 (**7**): 074301. DOI: 10.1088/1674-1056/abf91d

Radiation force and torque on a two-dimensional circular cross-section of a non-viscous eccentric layered compressible cylinder in acoustical standing waves

F G Mitri
Chin. Phys. B, 2021, 30 (**2**): 024302. DOI: 10.1088/1674-1056/abbbd9

Enhancement effect of cumulative second-harmonic generation by closed propagation feature of circumferential guided waves

Guang-Jian Gao(高广健), Ming-Xi Deng(邓明晰), Ning Hu(胡宁), Yan-Xun Xiang(项延训)
Chin. Phys. B, 2020, 29 (**2**): 024301. DOI: 10.1088/1674-1056/ab628d

Response features of nonlinear circumferential guided wave on early damage in inner layer of a composite circular tube

Ming-Liang Li(李明亮), Liang-Bing Liu(刘良兵), Guang-Jian Gao(高广健), Ming-Xi Deng(邓明晰), Ning Hu(胡宁), Yan-Xun Xiang(项延训), Wu-Jun Zhu(朱武军)
Chin. Phys. B, 2019, 28 (**4**): 044301. DOI: 10.1088/1674-1056/28/4/044301

Review on second-harmonic generation of ultrasonic guided waves in solid media (I):Theoretical analyses

Wei-Bin Li(李卫彬), Ming-Xi Deng(邓明晰), Yan-Xun Xiang(项延训)
Chin. Phys. B, 2017, 26 (**11**): 114302. DOI: 10.1088/1674-1056/26/11/114302

Characterization of inner layer thickness change of a composite circular tube using nonlinear circumferential guided wave: A feasibility study*

Ming-Liang Li(李明亮)[1], Guang-Jian Gao(高广健)[2], and Ming-Xi Deng(邓明晰)[1,†]

[1] *College of Aerospace Engineering, Chongqing University, Chongqing* 400044, *China*
[2] *Army Logistics University, Chongqing* 401331, *China*

(Received 12 December 2020; revised manuscript received 27 January 2021; accepted manuscript online 2 February 2021)

The feasibility of using the nonlinear effect of primary circumferential guided wave (CGW) propagation for characterizing the change of inner layer thickness of a composite circular tube (CCT) has been investigated. An appropriate mode pair of the fundamental and double-frequency CGWs (DFCGWs) has been selected to enable the second harmonics of primary wave mode in the given CCT to accumulate along the circumferential direction. When changes in the inner layer thickness (described as the equivalent inner layer thickness) take place, the corresponding nonlinear CGW measurements are conducted. It is found that there is a direct correlation between change of equivalent inner layer thickness of the CCT and the relative acoustic nonlinearity parameter ($\Delta\beta$) measured with CGWs propagating through one full circumference, and that the effect of second-harmonic generation (SHG) is very sensitive to change in the inner layer thickness. The experimental result obtained demonstrates the feasibility for quantitatively assessing the change of equivalent inner layer thickness in CCTs using the effect of SHG by primary CGW propagation.

Keywords: circumferential guided wave (CGW), second-harmonic generation (SHG), inner layer thickness, composite circular tube

PACS: 43.35.+d, 43.25.+y, 43.20.Mv **DOI:** 10.1088/1674-1056/abe234

1. Introduction

The composite circular tubes (CCTs), widely used in engineering industries, generally serve in complicated stress and corrosive environments of transporting substances, resulting in damage occurrence or minor thickness change in their inner layers.[1,2] In order to ensure the safe operation of the CCT structures, it is of great significance to study how to accurately monitor a minor change in its inner layer thickness.

Ultrasonic guided wave technique provides an effective means for detecting and inspecting structural components, but are invalid in characterizing material degradation or monitoring minor changes prior to crack initiation.[3,4] In contrast, the nonlinear ultrasonic technique has been proven to be more sensitive and efficient than the linear one for quantitatively characterizing material degradation or minor change. For accurately assessing the changing aspects of material microstructures (e.g., damage or degradation), the investigations of nonlinear ultrasonic guided waves have been drawn much attention in the recent two decades.[5] Deng *et al.* conducted the investigations of second-harmonic generation (SHG) of primary (fundamental frequency) guided wave propagation in solid plates, and found that the second harmonics may have a cumulative growth effect along propagation distance.[6,7] Subsequently, a series of theoretical and experimental investigations of nonlinear ultrasonic guided waves have been conducted, which revealed the physical mechanism of SHG of primary guided wave propagation, and meanwhile provided some effective techniques for analyzing and measuring second harmonics.[8–13] It has been experimentally verified that a minor change in material (e.g., degradation or fatigue) could be quantitatively assessed using the relative acoustic nonlinearity parameter as measured with second harmonics.

As a kind of elementary guided wave mode that propagates along the circumference of the circular tubes, the path of circumferential guided wave (CGW) propagation is closed, which has provided an efficient means for detecting radial cracks, pitting corrosion, and longitudinal defects in the CCT structures. The investigations of nonlinear effect of CGW propagation have been drawn much attention recently.[14–19] Considering the fact that the nonlinear effect of CGWs has been successfully used to evaluate accumulated damage in a single layer circular tube,[18] it is necessary to confirm whether the cumulative SHG effect of CGWs can be used to quantitatively characterize a minor change in the inner layer thickness of a given CCT. For this purpose, this study reports an investigation focusing on the feasibility of using the nonlinear effect of primary CGW propagation for characterizing the minor change in the inner layer thickness of a CCT.

*Project supported by the National Natural Science Foundation of China (Grant Nos. 12074050, 11834008, and 11704410).
†Corresponding author. E-mail: dengmx65@yahoo.com
© 2021 Chinese Physical Society and IOP Publishing Ltd

2. Theoretical considerations

The two-dimensional model with Lagrangian cylindrical coordinates (r, θ) for analyzing nonlinear CGW propagation in a CCT is illustrated in Fig. 1, where the materials of the inner layer (layer 1) and outer layer (layer 2) are assumed to be isotropic, homogeneous and dispersionless with no attenuation.

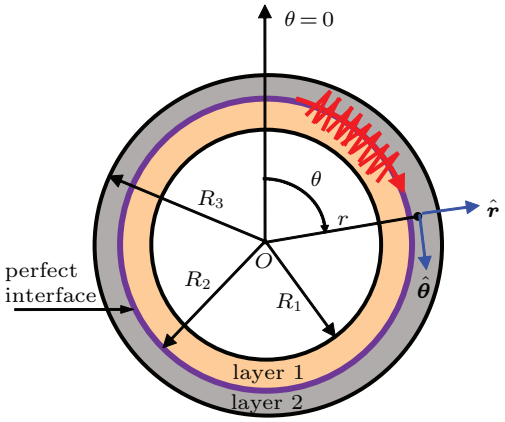


Fig. 1. Two-dimensional model with Lagrangian cylindrical coordinates (r, θ) for nonlinear CGW propagation in a CCT.

For the case of the CCT with a perfect interface, the mechanical conditions at the interface $r = R_2$ can be expressed as[16,19]

$$\begin{aligned} &P_{(1)rr} = P_{(2)rr}, \quad P_{(1)\theta r} = P_{(2)\theta r}, \\ &U_{(1)r} = U_{(2)r}, \quad U_{(1)\theta} = U_{(2)\theta}, \end{aligned} \tag{1}$$

where $P_{(i)rr} = \bar{\boldsymbol{r}} \cdot \boldsymbol{P}_{(i)} \cdot \bar{\boldsymbol{r}}$ and $P_{(i)\theta r} = \bar{\boldsymbol{\theta}} \cdot \boldsymbol{P}_{(i)} \cdot \hat{\boldsymbol{r}}$ are, respectively, the normal (radial) and shear (circumferential) components of the stress tensor $\boldsymbol{P}_{(i)}$ (i= 1, 2); $U_{(i)r}$ and $U_{(i)\theta}$ are the components of the displacement field $\boldsymbol{U}_{(i)}$; $\bar{\boldsymbol{r}}$ and $\bar{\boldsymbol{\theta}}$ are, respectively, the unit vectors along the radial and circumferential directions; the subscript number $i = 1$ or 2 corresponds to layer 1 or 2 in Fig. 1. The free stress boundary conditions at the inner and outer surfaces $r = R_1$ and $r = R_3$ are formally written as[16,19]

$$P_{(1)rr} = P_{(1)\theta r} = 0\big|_{r=R_1}, \quad P_{(2)rr} = P_{(2)\theta r} = 0\big|_{r=R_3}. \tag{2}$$

When a primary CGW mode (with the angular frequency ω and the order l) propagating clockwise along the circumference of the CCT is considered, the solution of the corresponding displacement field in each layer can be written as $U^{(l)}_{(i)q}(r)\exp[\mathrm{j}n^{(\omega,l)}\theta - \mathrm{j}\omega t]$ ($q = r$ or θ), where $n^{(\omega,l)} = \omega R_3/c_{\mathrm{p}}^{(\omega,l)}$ is the dimensionless angular wave number of the lth CGW mode, and $c_{\mathrm{p}}^{(\omega,l)}$ is the corresponding phase velocity. The dispersion equation of the primary lth CGW mode can be obtained from the mechanical boundary conditions, and can formally be given as[14,20]

$$\left|\boldsymbol{M}[\rho_{(i)}, \lambda_{(i)}, \mu_{(i)}, c_p^{(\omega,l)}, \omega, R_{(j)}]\right| = 0, \tag{3}$$

where $\rho_{(i)}$, $\lambda_{(i)}$, and $\mu_{(i)}$ ($i = 1$, 2) are the mass density and second-order elastic constants of material of the ith circular layer, and $R_{(j)}$ ($j = 1$, 2, or 3) denote the radius of the CCT; $\boldsymbol{M}[\ldots]$ is the coefficient matrix of the boundary condition equations. Similar to the process for solving the dispersion equation of primary CGW, the dispersion equation of double-frequency CGW (DFCGW) mode can readily be obtained through Eq. (3) just using 2ω instead of ω and $c_{\mathrm{p}}^{(2\omega,m)}$ instead of $c_{\mathrm{p}}^{(\omega,l)}$.[14–19] Here $c_{\mathrm{p}}^{(2\omega,m)}$ is the phase velocity of the mth DFCGW mode, and the corresponding dimensionless angular wave number is given by $n^{(2\omega,m)} = 2\omega R_3/c_{\mathrm{p}}^{(2\omega,m)}$. Obviously, when the materials of the CCT are given, the dispersion relations of primary CGWs, as well as DFCGWs, are dependent of the radius $R_{(j)}$.

When the primary lth CGW mode propagates along the circumference of the CCT shown in Fig. 1, within the second-order perturbation, the bulk driving force of twice the fundamental frequency $\boldsymbol{F}_b^{(2\omega)} = \boldsymbol{F}[\boldsymbol{U}^{(l)}]$ inside the CCT, as well as the traction stress tensor of twice the fundamental frequency $\boldsymbol{P}_s^{(2\omega)} = \boldsymbol{P}[\boldsymbol{U}^{(l)}]$ on the interfaces/surfaces of the CCT, can be generated due to the convective nonlinearity and the inherent elastic nonlinearity of solid.[7,8,14] According to a modal analysis approach,[7,8,14] $\boldsymbol{F}_b^{(2\omega)}$ and $\boldsymbol{P}_s^{(2\omega)}$ are, respectively, assumed to be the bulk and surface sources for generation of a series of DFCGW modes within a second-order perturbation approximation. The sum of these DFCGW modes constitutes the second-harmonic field [denoted by $\boldsymbol{U}^{(2\omega)}(r,\theta)$] of the lth CGW mode, namely,

$$\boldsymbol{U}^{(2\omega)}(r,\theta) = \sum_m A_m(\theta)\boldsymbol{U}^{(2\omega,m)}(r), \tag{4}$$

where $A_m(\theta)$ is the expansion coefficient of the field function of the mth DFCGW mode [denoted by $\boldsymbol{U}^{(2\omega,m)}(r)$].[14]

On the basis of the reciprocity relation and the orthogonality of guided wave modes, the equation governing the expansion coefficient $A_m(\theta)$ can be expressed as[14]

$$\left(\frac{\partial}{\partial\theta} - \mathrm{j}n^{(2\omega,m)}\right)A_m(\theta) = \frac{1}{4P_{mm}}\left[f_m^{\mathrm{s}}(\theta) + f_m^{\mathrm{v}}(\theta)\right], \tag{5}$$

where P_{mm} is the average power flow (per unit width, perpendicular to the tube section) of the mth DFCGW mode. Here

$$f_m^{\mathrm{s}}(\theta) = 2\mathrm{j}\omega\sum_{i=1}^{2}\left\{\tilde{\boldsymbol{U}}_{(i)}^{(2\omega,m)}(r)\cdot\boldsymbol{P}_s^{(2\omega)}\right\}\cdot\bar{\boldsymbol{r}}\Big|_{r=R_i}^{r=R_{i+1}}, \tag{6}$$

$$f_m^{\mathrm{v}}(\theta) = 2\mathrm{j}\omega\sum_{i=1}^{2}\int_{R_i}^{R_{i+1}}\tilde{\boldsymbol{U}}_{(i)}^{(2\omega,m)}(r)\cdot\boldsymbol{F}_b^{(2\omega)}\mathrm{d}r \tag{7}$$

are the excitation functions due to the surface stress and bulk driving force, respectively.[14] The symbol $\sim$ in Eqs. (6) and (7) denotes the complex conjugate operation for the corresponding physical quantities.

For simplicity, the position of excitation source for the primary CGW is assumed to be at $\theta = 0$. The initial condition for generation of the mth DFCGW mode requires that $A_m(\theta)$ be zero when $\theta = 0$. $A_m(\theta)$ can formally be derived from Eq. (5) as follows:[14]

$$\begin{aligned} A_m(\theta) &= A_m \sin(\Delta n\theta)/\Delta n \\ &\quad \times \exp(\mathrm{j}\Delta n\theta) \times \exp[\mathrm{j}n^{(2\omega,m)}\theta], \\ A_m &= [f_m^{\mathrm{s}}(\theta) + f_m^{\mathrm{v}}(\theta)]/4P_{mm}, \end{aligned} \tag{8}$$

where $\Delta n = [n^{(\omega,l)} - n^{(2\omega,m)}/2]$ is used to describe the dispersion degree between the primary wave mode and the mth DFCGW component. When $\Delta n \neq 0$, there is a beat effect for the magnitude of the mth DFCGW component with the propagation circumference angle θ.[14] It is found that $A_m(\theta)$ in Eq. (8) can grow linearly with the circumferential angle θ when $A_m \neq 0$ and $\Delta n = 0$ (i.e., both the nonzero energy flux and the phase velocity matching are simultaneously satisfied). For this case, the second-harmonic field $U^{(2\omega)}(r,\theta)$ is mainly dependent on the mth double-frequency CGW mode, the magnitude of the mth DFCGW component will grow linearly along the tube circumference and it has the following form:

$$A_m(\theta) = \frac{[f_m^{\mathrm{s}}(\theta) + f_m^{\mathrm{v}}(\theta)]}{4P_{mm}}\theta \exp[\mathrm{j}n^{(2\omega,m)}\theta]. \tag{9}$$

For a given CCT, the mode pair of CGW can be selected to ensure $\Delta n = 0$ or $\Delta n \to 0$. Thus, the mth DFCGW component will grow along the circumference of the CCT, and an obvious second-harmonic signal by the primary CGW propagation (mainly determined by the mth DFCGW component due to its cumulative growth with θ) can be observed.[14–16] When a minor change in the inner layer thickness of the CCT takes place (e.g., induced by corrosion), it is expected that the second-harmonic signals of the primary CGW mode will be influenced by the following aspects. First, the dispersion relation of CGWs in Eq. (3) will be affected. For the mode pair selected, the phase velocity matching condition $\Delta n = 0$ or $\Delta n \to 0$ may not be satisfied exactly when a change in inner layer thickness takes place. This will remarkably influence the efficiency of SHG by lth primary CGW propagation (reflected through the factor $\sin(\Delta n\theta)/\Delta n$ in Eq. (8). Second, change in the inner layer thickness of the CCT can provide different acoustic field features for the primary CGW mode. This will also influence the magnitude of $A_m(\theta)$ since $f_m^{\mathrm{s}}(\theta)$ and $f_m^{\mathrm{v}}(\theta)$ in Eqs. (8) and (9) are proportional to the square of the amplitude of the primary CGW mode.[14–16]

The above analyses demonstrate the feasibility that a minor change in the inner layer thickness of the given CCT may be quantitatively characterized by means of the effect of SHG of primary CGW propagation, specifically, by using the relative acoustic nonlinearity parameter β as measured with the second harmonic generated by primary guided wave propagation.

3. Experimental examinations

As analyzed in Section 2, for a given CCT with initial status, an appropriate mode pair of the primary and double-frequency CGW modes can be selected to enable that the second harmonics of primary CGW accumulates along the circumference of the CCT.[14] Thus, the magnitude of second harmonic generated by the primary CGW propagation, closely associated with the radius $R_{(j)}$ of the CCT, can be effectively determined and used to define the acoustic nonlinearity parameter β.[16] Theoretically, β is an intrinsic material parameter that describes the degree of nonlinearity of and the minor change in material. It can be expected that a minor change in the inner layer thickness of the CCT may be quantitatively assessed with β as measured with the second harmonics generated by primary CGW propagation. The experimental examinations shown below will positively confirm this expectation.

The initial radii of the examined CCT in Fig. 1 are $R_1 =$ 95.5 mm, $R_2 = 98.5$ mm, $R_3 = 106.5$ mm, and its materials from inner layer to outer one in order are 316L stainless steel and X65 pipeline steel, where the material parameters are listed in Table 1.

Table 1. The material parameters of the CCT.

Material	Mass density ρ (10^3 kg/m^3)	Longitudinal wave velocity c_{L} (km/s)	Shear wave velocity c_{T} (km/s)	3rd order elastic constants (GPa)		
				A	B	C
316L stainless steel	7.980	5.660	3.080	–720	–230	180
X65 pipeline steel	7.850	6.010	3.210	18	–266	–712

For simplicity, the CCT materials are assumed to be isotropic and homogeneous with no attenuation and no dispersion. The dispersion curves for the primary and double-frequency CGWs in the CCT with initial radii are shown in Fig. 2. For observation of cumulative SHG by primary CGW propagation, the specific mode pair (denoted by point P in Fig. 2) is selected, where the driving frequency is $f =$ 0.62 MHz (see vertical dotted line V in Fig. 2). The contribution of the other DFCGW modes to the second harmonic field generated is negligible due to the mismatching of their phase velocities with $c_P^{(\omega,l)}$ of point P in Fig. 2.

The schematic diagram of the experimental setup is illustrated in Fig. 3. The wedge transducer Tx, consisting of the plexiglas wedge (with an oblique angle α) and the longi-

tudinal wave transducer (V401, Panametrics Inc.), is used to generate the primary CGW mode desired (point P in Fig. 2), and the wedge transducer *Rx*, consisting of the same plexiglas wedge and the longitudinal wave transducer (V403, Panametrics Inc.), is used to receive the primary CGW mode (point *P*) and its second-harmonic signals.[18] The oblique angle α is determined by $\alpha = \sin^{-1}(c_{\rm L}/c_{\rm P})$, where $c_{\rm P}$ is the linear phase velocity of the circumferential guided wave (point *P*) and $c_{\rm L}$ is the longitudinal wave velocity of the wedge material, which is measured to be $c_{\rm L} = 2.688$ km/s. The two wedges of *Tx* and *Rx* are face-to-face positioned with a separation of $L = 140$ mm and permanently glued onto the outer surface of the CCT with the room-temperature epoxy resin adhesive (JC-311), where the longitudinal wave transducer V401 or V403 can readily be assembled onto or removed from the plexiglas wedge with bolts (see Fig. 3).

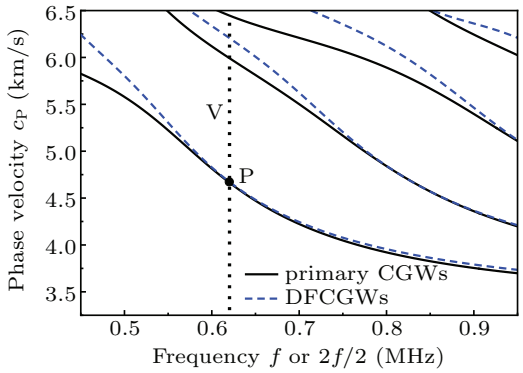


Fig. 2. Phase velocity curves of CGWs in the CCT.

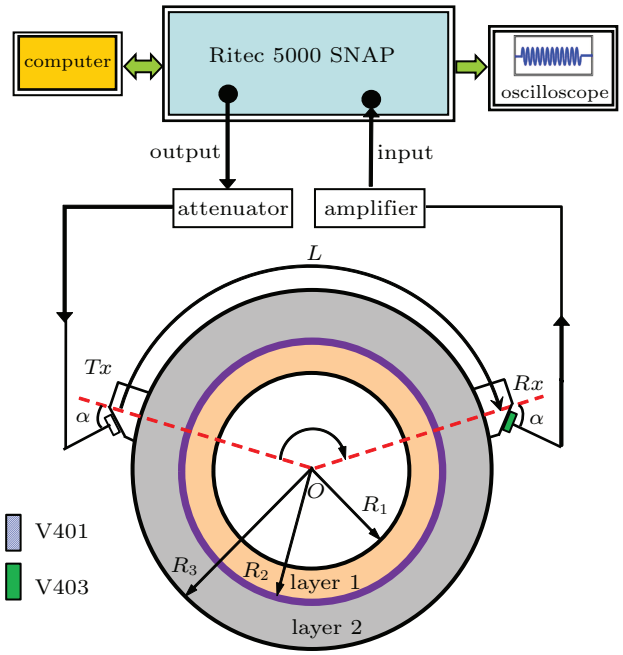


Fig. 3. Schematic diagram of experimental setup.

In the experimental measurements, the transducer *Tx* is always driven by a 40-cycle Hanning windowed sinusoidal tone-burst voltage (provided by the Ritec SNAP system, Ritec Inc.), whose carrier frequency is set to be 0.62 MHz (corresponding to the vertical line V in Fig. 2). The wedge transducer *Rx* successively receives two clear original time-domain signals [i.e., A and B in Fig. 4(a)] propagating in the CCT with the initial status. The group delay of the primary CGW mode (point P in Fig. 2; $c_{\rm g}^{\rm (P)} = 2.398$ km/s) along one full circumference of the examined CCT is theoretically calculated to be $2\pi R_3/c_{\rm g}^{\rm (P)} = 279.05$ μs, which is very close to the group delay $\Delta t = 276.63$ μs between the signals A and B (RE 0.867%). It is convinced that the signals A and B are certainly the CGW modes (point P) desired, and their corresponding propagation paths along the CCT shown in Fig. 3 are, respectively, L and $L+2\pi R_3$. For enhancing signal-to-noise ratio, a Hanning window with an appropriate width is, respectively, used to modulate the signal A or B, and then the corresponding signal C or signal D is obtained [see the blue waveform in Figs. 4(b) or 4(c)]. Through a band-pass digital filtering processing for the signal C or D, the corresponding second-harmonic signal of the primary CGW mode (point P) is clearly shown in Fig. 4(c).

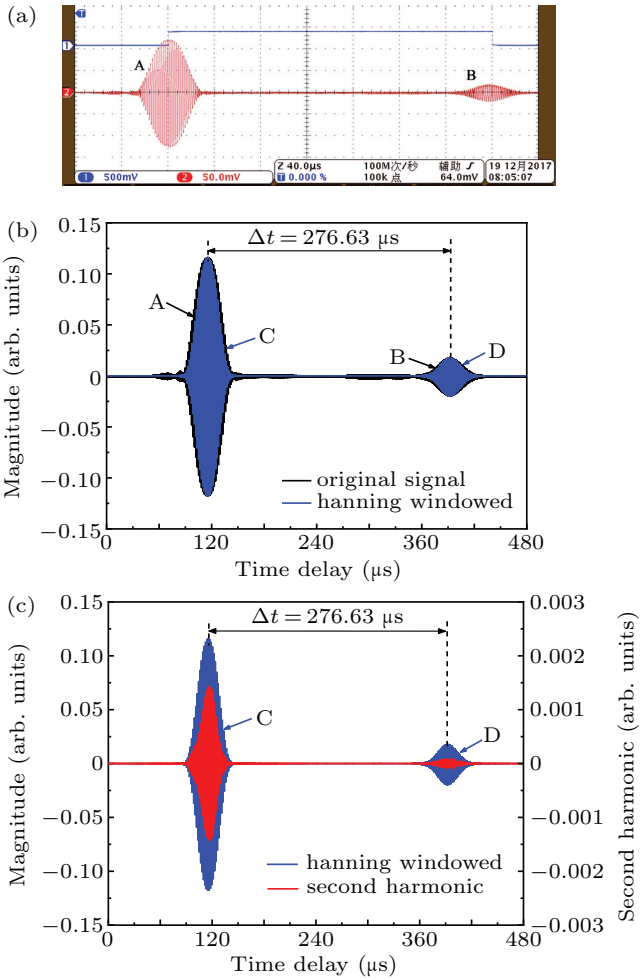


Fig. 4. Time-domain signals received by *Rx*: (a) oscilloscope display diagram, (b) original and Hanning windowed signals, (c) second-harmonic signals obtained by digital filtering processing.

The amplitude-frequency curves of the signals C and

D are shown in Fig. 5, through which the corresponding fundamental-frequency ($f = 0.62$ MHz) and second-harmonic ($f = 1.24$ MHz) amplitudes of the primary CGW (point P) propagation, denoted by A_f and A_{2f}, can readily be determined. Considering the fact that $\beta = A_{2f}/A_f^2$ is a measure of the acoustic nonlinearity parameter relative to its initial value and is proportional to the absolute acoustic nonlinearity parameter, for simplicity, β can directly be used as the acoustic nonlinearity parameter for material/structure evaluation.[7–10] The specified CGW mode pair (see point P in Fig. 2) is selected on this investigation, thus A_f is the value of the measured amplitude of the primary CGW mode at the fundamental frequency 0.62 MHz, while A_{2f} is the value of the measured amplitude of the DFCGW mode at the double frequency 1.24 MHz.

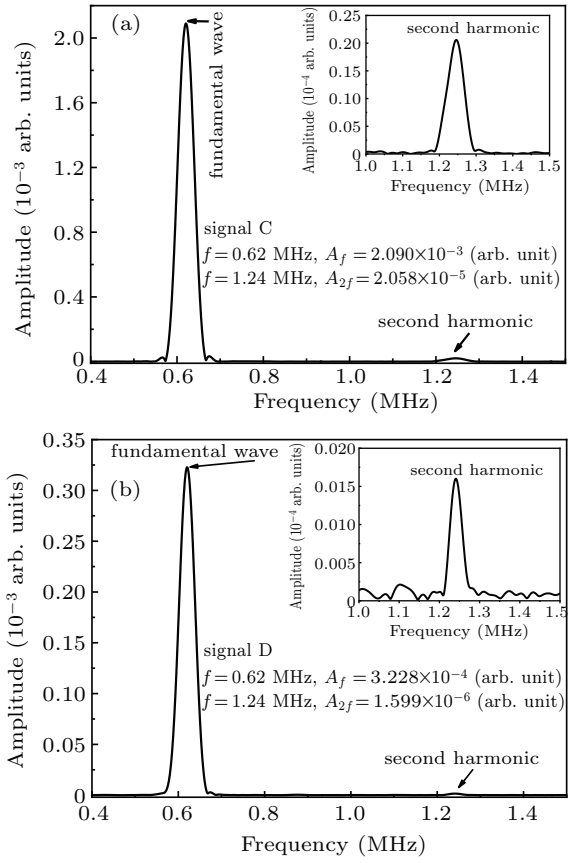


Fig. 5. Amplitude-frequency curves of the signals C and D in Fig. 4: (a) signal C, and (b) signal D.

Based on the values of A_f and A_{2f} given in Figs. 5(a) and 5(b), the acoustic nonlinearity parameter of the signals C and D are, respectively, calculated to be $\beta_C = 4.712$ (arb.unit), $\beta_D = 15.343$ (arb.unit). Generally, the origin of β_C includes the three aspects: the nonlinear contributions from the wedge transducers *Tx* and *Rx*, and the nonlinearity of the primary CGW (point P) propagation through the path *L*,[21] while the origin of β_D is the same as that of β_C except the nonlinear contribution through different path (i.e., $L + 2\pi R_2$). The fact of $\beta_D > \beta_C$ confirms that the second harmonic of the primary CGW mode (point P) grows along the tube circumference. Thus, the acoustic nonlinearity parameter for CGW propagation can be defined as $\Delta\beta = \beta_D - \beta_C$, which can completely removes the nonlinear influences arising from the wedge transducers themselves, the coupling interface between the wedge transducers and the specimen, and the ultrasonic instrument used. Clearly, the parameter $\Delta\beta$ characterizes the nonlinearity of the primary CGW mode (point P) propagating through one full circumference (i.e., $2\pi R_3$) of the given CCT.

Next we will focus on investigating the relationship of $\Delta\beta$ versus the change in the equivalent inner layer thickness of the given CCT. The inner surface of the CCT is covered by the copper foil tapes (40 mm width and 250 mm length) repeatedly at the same position of the inner layer, where the signal layer tape thickness is about 53 μm. The copper foil tapes on inner will modify the geometric parameters of the CCT, and are considered as the changes of equivalent inner layer thickness, where the change in the equivalent inner layer thickness in the CCT is denoted by the layer number of the copper foil tape, denoted by M. The CCT with the initial status is represented by $M = 0$. After pasted copper foil tape on the inner layer, the specimen examined is taken onto the measurement system shown in Fig. 3 for ultrasonic measurements of amplitude- frequency curves similar to that shown in Figs. 4 and 5. Based on the amplitude-frequency curves measured, the acoustic nonlinearity parameter for CGW propagation (i.e., $\Delta\beta = \beta_D$–β_C) for the given layer number M of the copper foil tape can readily be calculated.

Table 2. Values of β_C, β_D as well as $\Delta\beta$ and its normalized values versus initial status ($M = 0$) with different M.

M	β_C (arb. units)	β_D (arb. units)	$\Delta\beta = \beta_D - \beta_C$ (arb. units)	Normalized $\Delta\beta$
0	4.712	15.343	10.631	1.000
1	4.751	15.171	10.420	0.980
2	4.894	15.020	10.126	0.952
3	5.016	14.756	9.740	0.916
4	5.058	14.434	9.376	0.882
5	4.855	14.567	9.712	0.914
6	4.733	13.818	9.085	0.855
7	4.801	13.521	8.720	0.820
8	4.603	12.417	7.814	0.735
9	4.671	12.050	7.378	0.694

By pasting the copper foil tapes on the inner surface of the CCT and taking ultrasonic measurements repeatedly until $M = 9$, the $\Delta\beta$ for CGW propagation versus different layers of copper foil tape M can be obtained. Table 2 presents $\beta_C = A_{2f}/A_f^2\big|_{\text{signal C}}$ and $\beta_D = A_{2f}/A_f^2\big|_{\text{signal D}}$ for the signals C and D similar to that shown in Fig. 5, as well as $\Delta\beta$ and its normalized values versus initial status ($M = 0$). Data of the normalized amplitudes A_{f-C} and A_{f-D} of signal C and D versus M are shown in Fig. 6. The amplitudes A_{f-C} and A_{f-D}

of the lth primary CGW mode almost keep unchanged, and its relative change rates are within 3%. Obviously, the linear property of primary CGW propagation is not suitable for accurately monitoring the changes of equivalent inner layer thickness in the CCT.

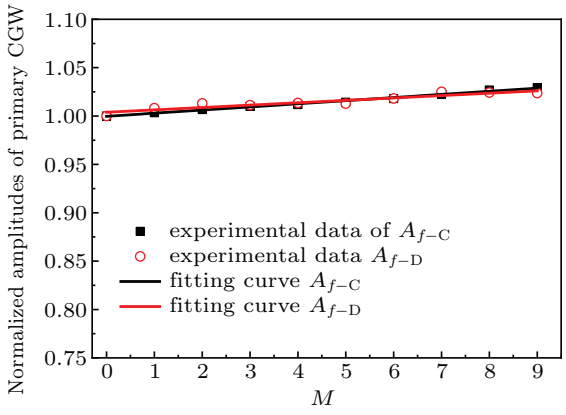


Fig. 6. Data of the normalized amplitudes A_{f-C} and A_{f-D} of signals C and D versus M.

According to Table 2, under different M, the data of normalized $\Delta\beta$ for CGW propagation through one full circumference are shown in Fig. 7. Clearly, the effect of SHG of primary CGW propagation is sensitive to the changes in the equivalent inner layer thickness (characterized by the layers of copper foil tape M) in the given CCT. It should be noted that the cumulative second harmonic, generated by closed propagation features of CGWs, has a remarkable advantage compared to other guided waves for accurately characterizing the change of inner layer thickness.[22]

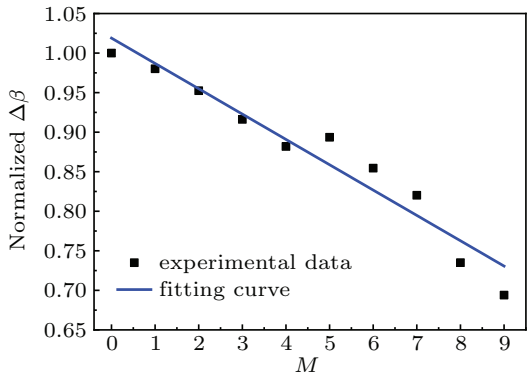


Fig. 7. Data of normalized $\Delta\beta$ versus M.

The above experimental examinations show that the effect of SHG by primary CGW propagation is very sensitive to change in the equivalent inner layer thickness in the given CCT. The experimental results validate the feasibility that the equivalent inner layer thickness of the CCT can be accurately evaluated with $\Delta\beta$.

4. Conclusions

This study has demonstrated the feasibility that the quantitative assessment of the change of equivalent inner layer thickness can be conducted by the acoustic nonlinearity parameter of primary CGW propagation through one full circumference. With the selection of appropriate mode pair of fundamental and double frequency CGWs in the given CCT, the second harmonics by primary CGW can accumulate along circumferential direction. When the equivalent inner layer thickness changes, the corresponding ultrasonic measurements are conducted where a pair of wedge transducers are used to generate the primary wave desired and to receive its fundamental-frequency and second-harmonic amplitudes on the outside surface of the CCT. Based on the values of the fundamental-frequency and second-harmonic amplitudes measured, the acoustic nonlinearity parameter for CGW propagation through one full circumference of the examined CCT can be determined. The experimental results show that the acoustic nonlinearity parameter for CGW propagation is very sensitive to the changes of equivalent inner layer thickness. The relationship between the acoustic nonlinearity parameter $\Delta\beta$ measured via the closed propagation features of CGWs and the layer of copper foil tape M provides a promising potential for accurately characterizing the change of inner layer thickness of the tested CCT.

References

[1] Wang H, Han J amd Zhang H 2013 *Appl. Mech. Mater.* **278** 487
[2] Iris R 2005 *World Oil* **226** 69
[3] Nagy P B 1998 *Ultrasonics* **36** 375
[4] Muller M, Sutin A, Guyer R and Talmant M 2006 *J. Acoust. Soc. Am.* **118** 3946
[5] Chillara V, Lissenden C 2016 *Opt. Eng.* **55** 011002
[6] Deng M 1996 *Jpn. J. Appl. Phys.* **35** 4004
[7] Deng M 1999 *J. Appl. Phys.* **85** 3051
[8] Lima W, Hamilton M 2003 *J. Sound Vib.* **265** 819
[9] Deng M, Wang P and Lv X 2005 *Appl. Phys. Lett.* **86** 124104
[10] Muller M, Kim J, Qu J and Jacobs L 2010 *J. Acoust. Soc. Am.* **127** 2141
[11] Matsuda N, Biwa S 2014 *J. Nondestruct. Eval.* **33** 169
[12] Deng M X and Xiang Y X 2010 *Chin. Phys. B* **19** 114302
[13] Zhao J, Chillara V, Ren B, Cho H and Qiu J 2016 *J. Appl. Phys.* **119** 064902
[14] Gao G, Deng M and Li M 2015 *Acta Phys. Sin.* **64** 184303 (in Chinese)
[15] Li M, Deng M, Zhu W and Gao G 2016 *Chin. Phys. Lett.* **33** 124301
[16] Li M, Deng M, Gao G and Chen H 2017 *Chin. Phys. Lett.* **34** 064302
[17] Li M, Deng M, Gao G and Xiang Y 2017 *Ultrasonics* **82** 171
[18] Deng M, Gao G, Xiang Y and Li M 2017 *Ultrasonics* **75** 209
[19] Li M, Deng M, Gao G and Xiang Y 2018 *J. Sound Vib.* **421** 234
[20] Rose J L 1999 *Ultrasonic Waves in Solid Media* (Cambridge: Cambridge University Press)
[21] Deng M, Xiang Y and Liu L 2011 *J. Appl. Phys.* **109** 113525
[22] Gao G, Deng M, Hu N and Xiang Y 2020 *Chin. Phys. B* **29** 024301